

3,5-二硝基水杨酸铈的制备、热分解机理及非等温反应动力学

张 衡 赵凤起* 仪建华 张晓宏 胡荣祖 徐司雨

(西安近代化学研究所, 西安 710065)

摘要: 用 3,5-二硝基水杨酸和硝酸铈为原料, 制备了 3,5-二硝基水杨酸铈(CeDNS), 采用元素分析、X 射线荧光光谱和 FTIR 对其进行了表征。用 TG 和 DSC 以及变温固相原位反应池/傅立叶变换红外光谱(RS-FTIR)联用技术研究了 3,5-二硝基水杨酸铈的热分解机理, 对主放热反应的 DSC 峰进行了数学处理, 计算得到了动力学参数和动力学方程。结果表明, 3,5-二硝基水杨酸铈的分解反应共有 3 个阶段, 其中包括一个脱水吸热过程和一个主放热过程, 主分解反应发生在第 2 阶段, 主分解反应的表现活化能 E_a 与指前因子 A 分别为: $159.17 \text{ kJ} \cdot \text{mol}^{-1}$ 和 $10^{11.33} \text{ s}^{-1}$, 主分解阶段的反应机理服从 Avrami-Erofeev 方程($n=1/4$), 主分解反应的动力学方程为: $d\alpha/dt=10^{11.33} \times 4(1-\alpha)[- \ln(1-\alpha)]^{3/4} e^{-1.92 \times 10^4/T}$ 。

关键词: 3,5-二硝基水杨酸铈; 热分解机理; 非等温反应动力学

中图分类号: O614.33*2; O643

文献标识码: A

文章编号: 1001-4861(2009)05-0869-06

Preparation, Thermal Behavior and Nonisothermal Decomposition Reaction Kinetics of Cerium 3,5-dinitrosalicylate(CeDNS)

ZHANG Heng ZHAO Feng-Qi* YI Jian-Hua ZHANG Xiao-Hong HU Rong-Zu XU Si-Yu

(Xi'an Modern Chemistry Research Institute, Xi'an 710065)

Abstract: Cerium 3,5-dinitrosalicylate(CeDNS) was synthesized by using 3,5-dinitrosalicylic acid, sodium hydroxide and cerium nitrate as raw materials, and was characterized by elementary analysis, X-ray fluorescence and FTIR spectroscopy. The thermal decomposition mechanism and kinetic parameters of the decomposition reaction of CeDNS were investigated by means of TG/DSC and in situ condensed phase thermolysis/FTIR(RS-FTIR). The kinetic equation of decomposition reaction was obtained. The results show that the decomposition process of CeDNS has three stages and the main exothermic decomposition reaction occurs in the second process. The kinetic parameters of the main exothermic decomposition reaction are: $E_a=159.17 \text{ kJ} \cdot \text{mol}^{-1}$, $A=10^{11.33} \text{ s}^{-1}$. The kinetic equation can be expressed as: $d\alpha/dt=10^{11.33} \times 4(1-\alpha)[- \ln(1-\alpha)]^{3/4} e^{-1.92 \times 10^4/T}$.

Key Words: CeDNS; thermal decomposition mechanism; nonisothermal reaction kinetics

In recent years, lead salts as combustion catalysts have been added into double base propellants or RDX-CMDB propellants in order to adjust combustion properties of solid propellant. However, this type of compounds have higher toxicity. Therefore, much more attention has been paid to the development of lead-free

catalysts. The rare-earth compounds have good catalytic performance according to our previous studies^[1~2]. In order to make deeper insight into the action mechanism of the catalysts, it is essential to investigate their thermal decomposition behaviors and kinetics. In this paper, a new energetic compound CeDNS was prepared

收稿日期: 2008-12-22。收修改稿日期: 2009-02-22。

国家自然科学基金(No.20573098)资助项目。

*通讯联系人。E-mail: npecc@163.com

第一作者: 张 衡, 男, 25 岁, 硕士研究生; 研究方向: 催化材料, 含能材料。

and characterized. The thermal behavior and non-isothermal decomposition reaction kinetics were studied.

1 Experimental

1.1 Sample

All chemicals used in the synthesis were analytical-grade commercial products and were used without further purification. The title compound used in this work was prepared according to Refs.^[3,4]. The typical synthesis was as follows: an appropriate amount of 3,5-dinitrosalicylic acid (1 mmol) was added to the distilled water (20 mL), stirred and titrated with 20 mL aqueous solution of sodium hydroxide (2 mmol) at 60 °C until the pH value about 8 was reached. Then the solution of cerous nitrate (1 mmol) was added into the prepared mixture dropwise with stirring at 60 °C for about three hours, and a yellow precipitate was obtained. The precipitate was washed with distilled water and dried at 60 °C. The title compound was obtained and kept in a vacuum desiccator before use. The elemental analyses were performed on an Elementar Vario III EL elemental analyzer and the X-ray fluorescence analysis was performed on a S4 Pioneer X fluorescence spectrometer. IR spectra were recorded on a NEXUS 870 FT-IR spectrophotometer (Nicolet Instruments Co., USA) as KBr pellet (4 000 ~ 400 cm^{-1}). Elemental anal. (%), calcd. for CeDNS: C 20.95, H 0.75, N 6.98, O 35.91, Ce 34.91; Found: C 22.11, H 1.43, N 6.79, O 34.80, Ce 34.87; IR(KBr), σ/cm^{-1} : 1 680 cm^{-1} ($\nu_{\text{C=O}}$) and 2500~4 000 cm^{-1} ($\nu_{\text{O-H}}$) vanish, 1 575 cm^{-1} ($\nu_{\text{C=O}}^{\text{as}}$) and 1 424 cm^{-1} ($\nu_{\text{C=O}}^{\text{s}}$) appear, 1 603 cm^{-1} ($\nu_{\text{C=C}}$), 1 524 cm^{-1} ($\nu_{\text{NO}_2}^{\text{as}}$) and 1 339 cm^{-1} ($\nu_{\text{NO}_2}^{\text{s}}$) do not shift. According to the results of elementary analysis, X-ray fluorescence, FTIR spectroscopy, TG analysis and corresponding Refs.^[3-5], the structure of CeDNS is proposed as in Fig.1.

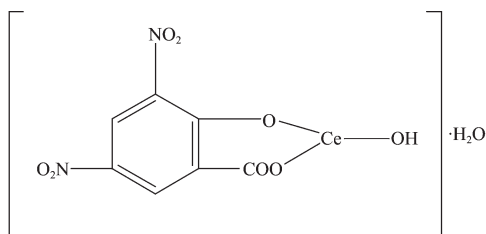


Fig.1 Structure of CeDNS

1.2 Equipment and conditions

TG-DTG and DSC curves under the condition of flowing nitrogen gas (purity, 99.999%; flow rate, 60 $\text{cm}^3 \cdot \text{min}^{-1}$; atmospheric pressure) were obtained by using a TA2950 thermal analyzer (TA Co., USA) and a TA 910S differential scanning calorimeter (TA Co., USA), respectively. The conditions of TG-DTG were as follows: about 1 mg sample; heating rate (β), 10 $^\circ\text{C} \cdot \text{min}^{-1}$. The conditions of DSC analyses were as follows: about 1 mg sample; heating rates (β), 5, 10, 15, 20 $^\circ\text{C} \cdot \text{min}^{-1}$, respectively.

Thermolysis/RS-FTIR measurements were conducted by using a NEXUS 870 FTIR spectrophotometer (Nicolet Instruments Co., USA) and *in situ* thermolysis cell (Xiamen University, China) with the temperature range of 20~450 $^\circ\text{C}$ and the heating rate of 10 $^\circ\text{C} \cdot \text{min}^{-1}$. KBr pellet samples (about 0.7 mg of CeDNS and 150 mg of KBr) were used. IR spectra of CeDNS in the range of 4 000~400 cm^{-1} were acquired by a DTGS detector at a rate of 11 files $\cdot \text{min}^{-1}$ and 8 scans $\cdot \text{file}^{-1}$ with a resolution of 4 cm^{-1} . The main gaseous products were determined by the T-jump/FTIR, which was used on a Nicolet 60 SXR FTIR spectrometer equipped with an MCT-A detector.

2 Results and discussion

2.1 Thermal behaviors

The typical TG-DTG and DSC curves of CeDNS are shown in Fig.2 and Fig.3, respectively. From Fig.2, one can find that there are three mass-loss stages in TG curve. The mass loss in the temperature range of 50~100 $^\circ\text{C}$ is attributed to the loss of adsorbent water. The first stage begins at about 100 $^\circ\text{C}$ and stops at 190 $^\circ\text{C}$, accompanied with 3.93% mass loss, which is in agreement with the theoretical value of the mass loss of 4.28%, corresponding to the mass of H_2O . The second stage begins at 250 $^\circ\text{C}$ and stops at 400 $^\circ\text{C}$, accompanied with 25.60% mass loss. The residue amounts are $\text{Ce}_2(\text{CO}_3)_3$ ^[5] and C. The third and fourth stages in the temperature range of 400~810 $^\circ\text{C}$ are attributed to the decomposition of $\text{Ce}_2(\text{CO}_3)_3$ and the oxidation of a few of carbon. At the end of decomposition process, the residue amounts to 33.20% ($\text{Ce}_2\text{O}_3 + \text{C}$). The DSC curve

(Fig.3) indicates that there are one endothermic peak and one exothermic peak, accompanied with the stages of TG curve, respectively. Additionally, from the DSC curves of CeDNS at different heating rates as shown in Fig.4, we can see that the peak temperature of DSC curve augments with the increase in the heating rate.

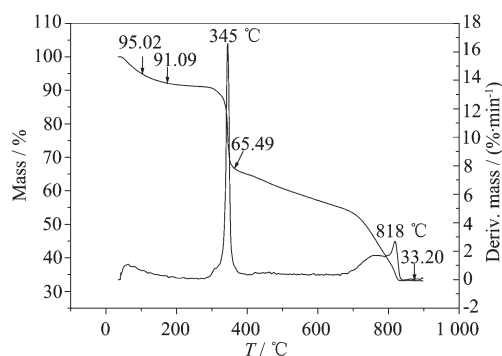


Fig.2 TG/DTG curves of CeDNS at a heating rate of $10\text{ }^{\circ}\text{C}\cdot\text{min}^{-1}$

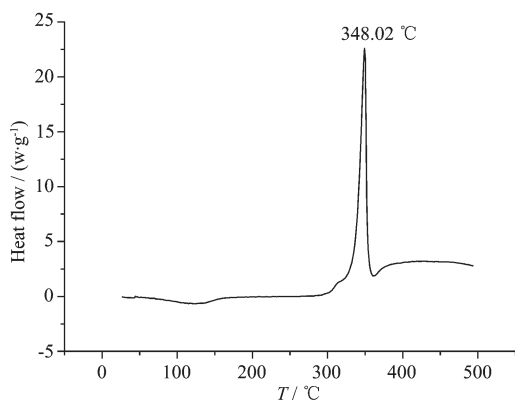
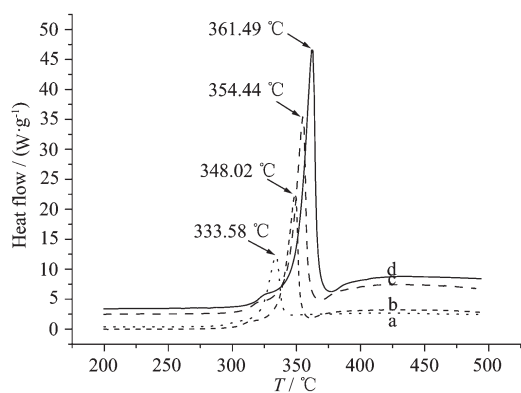


Fig.3 DSC curve of CeDNS at a heating rate of $10\text{ }^{\circ}\text{C}\cdot\text{min}^{-1}$



Heating rate ($^{\circ}\text{C}\cdot\text{min}^{-1}$): a 5; b 10; c 15; d 20.

Fig.4 DSC curves of CeDNS at different heating rates

The IR spectra of CeDNS at different temperatures and characteristic absorption peak intensity of the condensed phase decomposition products of CeDNS at different temperatures are shown in Fig.5 and 6, respectively. From Fig.5 and 6, one can find that the intensity of the 3421 cm^{-1} ($\nu_{\text{O-H}}$) weakens rapidly at $150\text{ }^{\circ}\text{C}$ and $300\text{ }^{\circ}\text{C}$, accompanied with the loss of H_2O and OH , respectively. The intensities of the 1575 cm^{-1} ($\nu_{\text{COO}}^{\text{as}}$), 1424 cm^{-1} ($\nu_{\text{COO}}^{\text{s}}$), 1529 cm^{-1} ($\nu_{\text{NO}_2}^{\text{as}}$) and 1339 cm^{-1} ($\nu_{\text{NO}_2}^{\text{s}}$) weaken rapidly in the temperature range of $250\sim350\text{ }^{\circ}\text{C}$. This indicates that the main decomposition process of the compound and the break of C-NO_2 bond occurs in the second stage. In addition, the intensity of the 2350 cm^{-1} strengthens rapidly in the temperature range of $250\sim350\text{ }^{\circ}\text{C}$ due to the appearance of CO_2 .

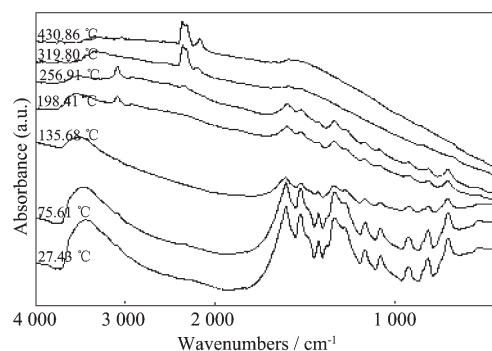


Fig.5 IR spectra of the condensed phase decomposition products of CeDNS at various temperatures

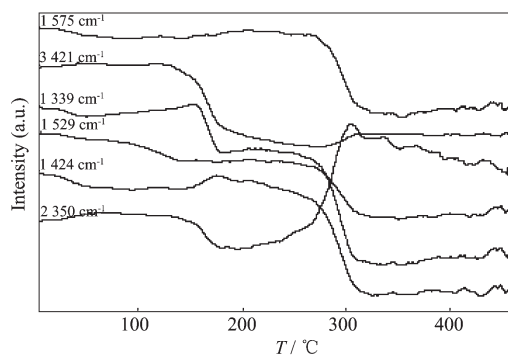
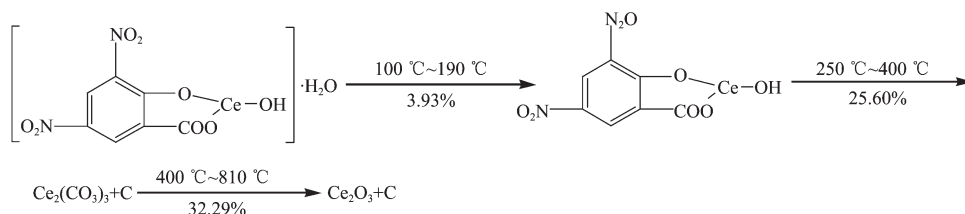


Fig.6 IR characteristic absorption peak intensity for the condensed phase decomposition products of CeDNS at different temperatures

On the basis of the above experimental results, the thermal decomposition mechanism of CeDNS can be expressed as:



2.2 Nonisothermal calculation kinetics

In order to obtain the most probable mechanism function and the corresponding kinetic parameters for

the main exothermic decomposition process of the compound, the following five integral methods and one differential method listed in Table 1 are employed^[6-13].

Table 1 Kinetic analysis methods and corresponding equations

Methods	Equations
General integral	$\ln[G(\alpha)/T^2] = \ln\{[A R/(\beta E)](1-2RT/E)\} - E/(RT)$ (1)
Mac Callum-Tanner	$\lg[G(\alpha)] = \lg[A E/(\beta R)] - 0.4828 E^{0.4357} - (0.449 + 0.217E)/(0.001T)(E \text{ in kcal} \cdot \text{mol}^{-1})$ (2)
Šatava-Šesták	$\lg[G(\alpha)] = \lg[A_s E_s/(\beta R)] - 2.315 - 0.4567 E_s/(RT)$ (3)
Agrawal	$\ln[G(\alpha)T^2] = \ln\{[A R/(\beta E)][1-2(RT/E)]/[1-5(RT/E)^2]\} - E/(RT)$ (4)
Flynn-Wall-Ozawa	$\lg\beta = \lg\{A E/[R G(\alpha)]\} - 2.315 - 0.4567 E/(RT)$ (5)
Kissinger	$\ln(\beta/T_p^2) = \ln(A_i R/E_i) - E_i/(RT_{p,i}), i=1,2,\dots,4$ (6)

In those equations, α is the fractional decomposition, T , the temperature(K) at time t ; T_0 , the initial point at which DSC curve deviates from the baseline; R , the gas constant; A , the pre-exponential factor; E , the apparent activation energy; β , the heating rate; $f(\alpha)$ and $G(\alpha)$ are the differential and integral

mechanism function, respectively; T_p , the peak temperature of DSC curve. The data needed for the equations of the integral and differential methods, i , α_i , β , T_i , $T_{p,i}$ ($i=1,2,3,\dots,50$), are obtained from the DSC curves and summarized in Table 2.

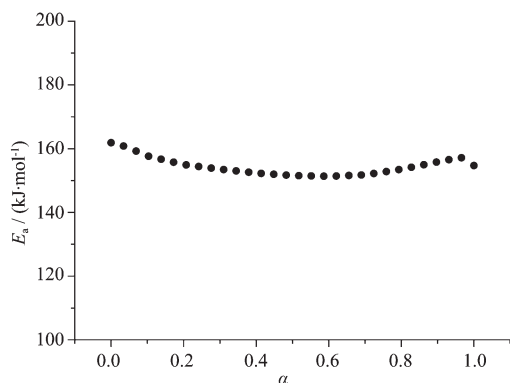
Table 2 Basic data for the main decomposition process of CeDNS

α	T / K				α	T / K			
	$5 \text{ K} \cdot \text{min}^{-1}$	$10 \text{ K} \cdot \text{min}^{-1}$	$15 \text{ K} \cdot \text{min}^{-1}$	$20 \text{ K} \cdot \text{min}^{-1}$		$5 \text{ K} \cdot \text{min}^{-1}$	$10 \text{ K} \cdot \text{min}^{-1}$	$15 \text{ K} \cdot \text{min}^{-1}$	$20 \text{ K} \cdot \text{min}^{-1}$
0.02	590.90	603.08	608.81	616.21	0.36	603.85	618.27	624.42	631.65
0.04	593.59	606.16	611.98	619.20	0.38	604.14	618.63	624.78	632.02
0.06	595.26	608.16	614.04	621.16	0.40	604.43	618.96	625.13	632.39
0.08	596.50	609.62	615.57	622.67	0.42	604.71	619.28	625.46	632.73
0.10	597.50	610.80	616.79	623.89	0.44	604.99	619.59	625.79	633.07
0.12	598.35	611.81	617.80	624.91	0.46	605.26	619.89	626.10	633.39
0.14	599.05	612.66	618.66	625.79	0.48	605.52	620.18	626.40	633.71
0.16	599.68	613.38	619.42	626.57	0.50	605.77	620.47	626.69	634.01
0.18	600.24	614.03	620.11	627.27	0.52	606.03	620.75	626.98	634.30
0.20	600.74	614.67	620.73	627.89	0.54	606.28	621.03	627.26	634.59
0.22	601.20	615.24	621.29	628.47	0.56	606.53	621.30	627.53	634.87
0.24	601.63	615.76	621.82	629.01	0.58	606.77	621.58	627.79	635.15
0.26	602.05	616.22	622.31	629.51	0.60	607.01	621.83	628.05	635.41
0.28	602.46	616.65	622.78	629.98	0.62	607.25	622.09	628.30	635.67
0.30	602.84	617.07	623.22	630.43	0.64	607.49	622.34	628.55	635.93
0.32	603.19	617.49	623.64	630.86	0.66	607.72	622.58	628.78	636.17
0.34	603.53	617.89	624.03	631.26	0.68	607.95	622.82	629.01	636.39

Continued Table 2

0.70	608.18	623.04	629.23	636.61	0.88	610.46	624.78	631.05	638.44
0.72	608.41	623.26	629.44	636.81	0.90	610.82	625.05	631.36	638.75
0.74	608.64	623.46	629.63	637.01	0.92	611.25	625.39	631.74	639.13
0.76	608.88	623.65	629.82	637.19	0.94	611.78	625.84	632.23	639.64
0.78	609.11	623.84	630.00	637.37	0.96	612.52	626.50	632.95	640.38
0.80	609.35	624.02	630.19	637.56	0.98	613.80	627.63	634.28	641.73
0.82	609.61	624.20	630.38	637.74	1.00	620.15	633.15	641.15	649.05
0.84	609.87	624.38	630.58	637.95					
0.86	610.16	624.57	630.80	638.18		$T_c=606.73$	$T_c=621.17$	$T_c=627.69$	$T_c=634.64$

The values of E_a were obtained by Ozawas method with changing from 0.02 to 1.00 and the E_a - α relation is show in Fig.7. It indicates that the activation energy of the decomposition process changes greatly by diverse levels with an increase in the conversion degree, except for the section of 0.10~0.90(α), in which activation

Fig.7 E_a - α curve obtained by Ozawas method

energy changes faintly, and it means that the decomposition mechanism of the process does not involve transference in essence, or the transference can be ignored. Therefore, it is feasible to study the reaction mechanism and kinetics in the section of 0.10~0.90(α).

Forty-one types of kinetic model functions in Ref. [6] and the original data tabulated in Table 2 are put into Eqs.(1)~(6), respectively, for calculations. The value of E_a , $\lg A$, linear correlation coefficient(r), and standard mean square deviation (Q) can be calculated on computer with linear least-squares method at various heating rates of 5, 10, 15, 20 K·min⁻¹. The most probable mechanism function is selected by better values of r and Q taken from Ref. [6]. The results satisfying the conditions mentioned above are listed in Table 3.

Table 3 Kinetic parameters obtained for the main decomposition process of CeDNS

Method	β / (K·min ⁻¹)	E_a / (kJ·mol ⁻¹)	$\lg A$ · s ⁻¹	r	Q
General Integral	5	164.49	11.82	0.999 8	0.001 7
	10	155.79	11.02	0.996 4	0.025 8
	15	155.01	10.99	0.996 6	0.024 6
	20	156.54	11.09	0.996 7	0.023 7
Mac Callum-Tanner	5	167.10	12.03	0.999 8	0.000 3
	10	158.57	11.24	0.996 8	0.004 9
	15	157.89	11.22	0.997 0	0.004 7
	20	159.55	11.32	0.997 1	0.004 5
Šatava-Šesták	5	165.95	11.95	0.999 8	0.000 3
	10	157.90	11.20	0.996 8	0.004 9
	15	157.25	11.19	0.997 0	0.004 7
	20	158.83	11.29	0.997 1	0.004 5
Agrawal	5	164.49	11.82	0.999 8	0.001 7
	10	155.79	11.02	0.996 4	0.025 8

Continued Table 3

	15	155.01	10.99	0.996 6	0.024 6
	20	156.54	11.09	0.996 7	0.023 7
Mean		159.17	11.33		
Flynn-Wall-Ozawa		153.43		0.998 2	0.000 7
Kissinger		151.04	10.61	0.997 9	0.003 9

The values of E_a and $\lg A$ obtained from nonisothermal DSC curves are in approximately agreement with the values calculated by Kissingers method and Ozawas method. Therefore, a conclusion can be drawn that the reaction mechanism of the main decomposition process of CeDNS is controlled by Avrami-Erofeev equation ($n=1/4$). Substituting $f(\alpha)$ with $4(1-\alpha)[- \ln(1-\alpha)]^{3/4}$, E_a with $159.17 \text{ kJ} \cdot \text{mol}^{-1}$ and A with $10^{11.33} \text{ s}^{-1}$ into Eq.(7):

$$\frac{d\alpha}{dt} = Af(\alpha)e^{-E_a/(RT)} \quad (7)$$

And the kinetic equation of the main decomposition reaction of CeDNS may be described as:

$$\frac{d\alpha}{dt} = 10^{11.33} \times 4(1-\alpha)[- \ln(1-\alpha)]^{3/4} e^{-1.92 \times 10^4/T} \quad (8)$$

3 Conclusions

(1) CeDNS was synthesized and the structure was determined as shown in Fig.1.

(2) The decomposition process of CeDNS is in three stages and the main decomposition reaction occurs in the second-stages. The mechanism of the thermal decomposition reaction of the compound could be described by the scheme shown in the text.

(3) The kinetics of the main decomposition reaction of the CeDNS has been investigated, and the kinetic model function in differential form, apparent activation energy, and pre-exponential constant of this reaction are $4(1-\alpha)[- \ln(1-\alpha)]^{3/4}$, $159.17 \text{ kJ} \cdot \text{mol}^{-1}$, $10^{11.33} \text{ s}^{-1}$, respectively.

References:

[1] SU Hang(苏航). *Thesis for the Master Degree of Xi'an*

Modern Chemistry Research Institute(西安近代化学研究所硕士学位论文). **1994**.

[2] SHAN Wen-Gang(单文刚). *Thesis for the Master Degree of Xi'an Modern Chemistry Research Institute*(西安近代化学研究所硕士学位论文). **1988**.

[3] SONG Xiu-Duo(宋秀铎), ZHAO Feng-Qi(赵凤起), XU Si-Yu(徐司雨), et al. *Chin. J. Expls. Propellants*. (Huozhayao Xuebao), **2006**, **29**(1):36~39

[4] Russell R. Jr. *Propellant Binders Cure Catalyst*. US4379903, **1983**.

[5] YI Jian-Hua(仪建华), ZHAO Feng-Qi(赵凤起), GAO Hong-Xu(高红旭), et al. *Chin. J. Expls. Propellants*. (Huozhayao Xuebao), **2007**, **30**:1~5

[6] HU Rong-Zu(胡荣祖), GAO Sheng-Li(高胜利), ZHAO Feng-Qi(赵凤起), et al. *Thermal Analysis Kinetics*(热分析动力学). Beijing: Science Press, **2008**.

[7] BI Cai-Feng(毕彩丰), XIAO Yan(肖艳), FAN Yu-Hua(范玉华), et al. *J. Rare Earths*(Xitu Xuebao), **2007**, **25**:1~4

[8] YI Jian-Hua(仪建华), ZHAO Feng-Qi(赵凤起), XU Si-Yu(徐司雨), et al. *Acta Phys. -Chim. Sin.*(Wuli Huaxue Xuebao), **2007**, **23**:1316~1320

[9] XU Kang-Zhen(徐抗震), MA Hai-Xia(马海霞), SONG Ji-Rong(宋纪蓉), et al. *J. Chin. Chem. Soc. (Zhongguo Huaxue Huizhi)*, **2007**, **54**:277~284

[10] ZHAO Feng-Qi(赵凤起), HU Rong-Zu(胡荣祖), GAO Hong-Xu(高红旭), et al. *J. Chin. Ordnance*(Zhongguo Binggong Xuebao), **2007**, **3**:68~70

[11] Hu R Z, Chen S P, Gao S L, et al. *J. Hazard. Mater.*, **2005**, **117**:103~110

[12] SONG Ji-Song(宋纪蓉), MA Hai-Xia(马海霞), HUANG Jie(黄洁), et al. *J. Chin. Chem. Soc. (Zhongguo Huaxue Huizhi)*, **2005**, **52**:1089~1094

[13] Jiao B J, Chen S P, Zhao F Q, et al. *J. Hazard. Mater.*, **2007**, **142**:550~554